The Astrophysical Journal, 808:18 (9pp), 2015 July 20 doi:10.1088/0004-637X/808/1/18

THERMAL ABSORPTION AS THE CAUSE OF GIGAHERTZ-PEAKED SPECTRA IN PULSARS AND MAGNETARS

Wojciech Lewandowski[1], Karolina Rożko[1], Jarosław Kijak[1], and George I. Melikidze[1,2]
[1] Institute of Astronomy, University of Zielona Gora, Szafrana 2, 65-516 Zielona Gora, Poland; boe@astro.ia.uz.zgora.pl
[2] Abastumani Astrophysical Observatory, Ilia State University, 3-5 Cholokashvili Ave., Tbilisi, 0160, Georgia
Received 2014 September 24; accepted 2015 May 22; published 2015 July 15

ABSTRACT

We present a model that explains the observed deviation of the spectra of some pulsars and magnetars from the power-law spectra that are seen in the bulk of the pulsar population. Our model is based on the assumption that the observed variety of pulsar spectra can be naturally explained by the thermal free–free absorption that takes place in the surroundings of the pulsars. In this context, the variety of the pulsar spectra can be explained according to the shape, density, and temperature of the absorbing media and the optical path of the line of sight across it. We have put specific emphasis on the case of the radio magnetar SGR J1745–2900 (also known as the Sgr A* magnetar), modeling the rapid variations of the pulsar spectrum after the outburst of 2013 April as due to the free–free absorption of the radio emission in the electron material ejected during the magnetar outburst. The ejecta expands with time and consequently the absorption rate decreases and the shape of the spectrum changes in such a way that the peak frequency shifts toward the lower radio frequencies. In the hypothesis of an absorbing medium, we also discuss the similarity between the spectral behavior of the binary pulsar B1259–63 and the spectral peculiarities of isolated pulsars.

Key words: ISM: general – ISM: supernova remnants – pulsars: general

1. INTRODUCTION

The gigahertz-peaked spectra (GPS) pulsars are those radio pulsars that show a broad maximum of the flux density at frequencies typically around one or a few GHz. This significantly distinguishes them from the bulk of the pulsar population. The radio spectra of pulsars can generally be described by a single power-law function, with an average spectral index that is in the range of about −1.4 to about −1.8, according to different analyses and investigated samples (e.g., Lorimer et al. 1995; Kramer et al. 1998; Maron et al. 2000; Bates et al. 2013). The distribution is also rather broad, with a standard deviation around one when a Gaussian distribution for the indices is adopted (Bates et al. 2013).

The first pulsars that indicate a turnover at high frequencies were identified by Kijak et al. (2007), and later Kijak et al. (2011a) named them "GPS pulsars." Kijak et al. (2011a) also indicated that the GPS pulsars tend to have peculiar environments, such as pulsar wind nebulae (PWN), dense H II regions, or SNRs. Therefore, it was suggested that the external influence accounts for the GPS phenomena rather than the peculiarities of the emission process. This statement was further strengthened by Kijak et al. (2011b) who demonstrated that the spectrum of the binary pulsar B1259–63 varies according to the pulsar's orbital phase.

Later, based on the available data Kijak et al. (2013) showed that two radio-magnetars (J1550–5418 and J1622–4950) can also be considered GPS sources since they show the turnovers at frequencies of about a few gigahertz. The number of known GPS pulsars is still growing and currently there are 11 such objects (Dembska et al. 2014), which seems to be a rather small population. However, recent statistical studies of the largest pulsar search surveys (Bates et al. 2013) indicate that the GPS pulsars can amount to up to several percent of the whole pulsar population. Thus we can expect to observe up to 200 pulsars showing the GPS phenomenon among over 2300 currently known pulsars. The reason why we currently observe only 11 GPS pulsars should rather be an observational selection effect. The spectra of GPS pulsars make them easier to be discovered at intermediate frequencies (around 1.4 GHz). However, not all discoveries are followed by observations at lower frequencies; therefore, the spectra of newly discovered pulsars usually remain unknown, which is partially caused by the relatively poor sensitivity (at least until recently) of the low frequency observations. In addition, the GPS pulsars, by definition, are weaker at sub-gigahertz frequencies. Fortunately, the situation has recently changed as a number of low frequency observatories (LOFAR, MWA, LWA) are becoming operational.

As we have already mentioned, the case of the binary pulsar B1259–63 is the key to understanding the origin of the GPS phenomenon in pulsars. For this case, Kijak et al. (2011b) suggested that the primary reason for the spectral turnover is the thermal free–free absorption of the pulsar radio emission in the strong stellar wind of the companion Be-star. Therefore, the pulsar motion along the elliptical orbit causes spectral evolution. While the pulsar remains far from the companion (where the stellar wind density is quite low) its spectrum is a usual, single power law. However, when the pulsar is approaching periastron, passing through the dense stellar wind, its spectrum displays GPS behavior. This effect has recently been modeled by Dembska et al. (2012), who have shown that the evolution of the spectrum can be explained by free–free absorption in the stellar wind. If the wind carries about $10^{-9}\,M_{\odot}$ yr^{-1} the mass-loss yields the electron density of about 10^5 electrons per cm^3 at the distance of 1 AU from the star. This density is enough to provide the observed absorption. Let us note that the pulsar approaches the star as close as 0.4 AU in the periastron.

Sieber (1973) was the first to propose that the thermal absorption in the interstellar medium caused low-frequency turnovers in pulsar spectra. However, it should be mentioned that the Vela pulsar, which has the highest turnover frequency

(with peak at about 600 MHz) quoted in that paper, is currently known to have a bow-shock PWN.

In the case of PSR B1259–63, the apparent cause of turnovers is the absorption in the dense stellar wind, while this is not the case for other GPS pulsars because they do not have stellar companions. However, as was mentioned above, the GPS pulsars tend to adjoin some peculiar environments where the matter density is much higher than that of the ISM. Thus the natural question arises, can the same process be responsible for the GPS phenomenon in all objects under consideration? We can distinguish three cases: first is the case of PSR B1259–63, which is expected to have a highly localized (within a few AU inside the orbit) environment with a high particle density and a high temperature (presumably of the order of several thousand kelvins); second, there is a vast interstellar space of very low electron density, which is relatively cold and causes low-frequency turnovers in pulsars; and finally, there are these peculiar pulsar surroundings, which are usually much larger in size than the PSR B1259–63 orbit, but much smaller and at the same time much denser than the interstellar free-electron clouds.

In this paper, we explore the possibility whether the thermal absorption in pulsar surroundings can indeed cause high-frequency turnovers in the GPS pulsars, as we proposed in Kijak et al. (2011b, 2013). Using the simplified model of such environments we estimate the domain of the parameters that are necessary to cause the thermal absorption of the pulsar radiation, as well as to change the pulsar spectrum in such a way that it becomes a GPS. The main parameters to be estimated are the size of the absorbing regions, the density, and temperature of electrons. Since, at present, it is extremely hard to measure these parameters (e.g., the electron temperature and distribution within PWNe or SNRs), we hope that our simulations at least give a rough estimate of what we expect, or rather what we need in order to explain the GPS pulsar spectra using the thermal free–free absorption.

2. THERMAL ABSORPTION AS THE CAUSE OF GPS

In our model, we consider the propagation of pulsar radio emission through the absorbing region (Kijak et al. 2011b, 2013). We assume that the intrinsic pulsar spectrum is a single power law with a spectral index equal or close to −1.8 (which is an average population value, Maron et al. 2000). In our models, we use the approximation of homogeneous electron density and uniform temperature since we need only rough estimations of the parameters. We assume that the absorption happens over a fraction of the pulsar's line of sight and that the optical path length is defined by the geometry.

2.1. The Model

The model is based on the formalism of the radiative transfer theory. For simplicity, we also assume the local thermal equilibrium approximation. Under such conditions, the radiative transfer equation has the following solution (Rohlfs & Wilson 2004):

$$I_\nu(s) = I_\nu(0)e^{-\tau_\nu(s)} + B_\nu(T)\left(1 - e^{-\tau_\nu(s)}\right), \quad (1)$$

where τ_ν is the optical depth, $B_\nu(T)$ is the Planck function and $I_\nu(0)$ is the incoming intensity (which, in our case, is the intrinsic emitted intensity). Assuming that the plasma is quasi-neutral and the electrons obey the thermal distribution, we obtain the optical depth in the following form (Rohlfs & Wilson 2004).

$$\tau_\nu = 3.014 \times 10^{-2}\left(\frac{T_e}{\mathrm{K}}\right)^{-3/2}\left(\frac{\nu}{\mathrm{GHz}}\right)^{-2}\left(\frac{\mathrm{EM}}{\mathrm{pc\ cm^{-6}}}\right)\langle g_{\mathrm{ff}}\rangle, \quad (2)$$

where EM is the Emission Measure ($\mathrm{EM} = \int N_e^2 dl$) and $\langle g_{\mathrm{ff}}\rangle$ is the Gaunt factor (see Rohlfs & Wilson 2004 for definitions). In the case of the free–free absorption and a uniform density profile the $\mathrm{EM} = N_e^2 d$, where d is simply the total thickness of the absorber.

Equations (1) and (2) as well as the geometrical length of the path that the radio waves follow through the absorbing region allows us to estimate the fraction of the flux that is absorbed during its passage through the medium. The value of the fraction depends on the physical parameters of the absorbing region, as well as on the wave frequency, i.e., the amount of the absorbed radiation obviously depends on the optical depth, which on its turn is frequency dependant. Applying results of the calculations of optical depth to the simulated (intrinsic) pulsar spectra, we can estimate the shape of "observed" spectra.

The simplest possible case to be considered is when the cloud of an absorbing electron-rich material is located anywhere between the pulsar and the observer. The cloud does not have to be close to the pulsar because, in our calculations, the position of the absorbing region along the line of sight does not matter. However, we are mostly interested in the cases where a cloud is located in the vicinity of a pulsar, thus the pulsars are somehow physically connected to the absorbers (e.g., PWNe, SNRs, or some other regions with heightened density).

The top and middle panels of Figure 1 show the simulated pulsar spectrum for the absorber whose thickness along the line of sight is 1.2 pc. The panels show the spectra obtained for various values of the electron temperature with the assumption that the electron number density is constant and equal to 100 $\mathrm{cm^{-3}}$ for the left panel, while for the right panel the electron number density equals 1000 $\mathrm{cm^{-3}}$. As can be seen in the panels, the amount of absorption obviously increases with decreasing temperature. For the lower density, the temperature should be considerably low (of the order of 100 K) to be able to affect the pulsar spectrum significantly and produce a turnover at gigahertz frequencies. At higher temperatures, the turnover frequency decreases below 1 GHz, approaching 100 MHz at temperatures of the order of a few thousand kelvins. Of course, the higher density translates into the higher optical depth (larger absorption) because, in the case of the free–free absorption, the depth depends on N_e^2. In this case, all of the simulated spectra show high frequency turnovers (above 1 GHz) with the spectrum peaking at frequencies close to 10 GHz for the coldest case (100 K).

The bottom panel of Figure 1 shows the simulated pulsar spectra for three different values of the geometrical length of the path (i.e., various thicknesses of absorbers) obtained for fixed values of both the electron density and the temperature. In this case, the values of the electron number density and the temperature have been set to 300 $\mathrm{cm^{-3}}$ and 500 K, respectively.

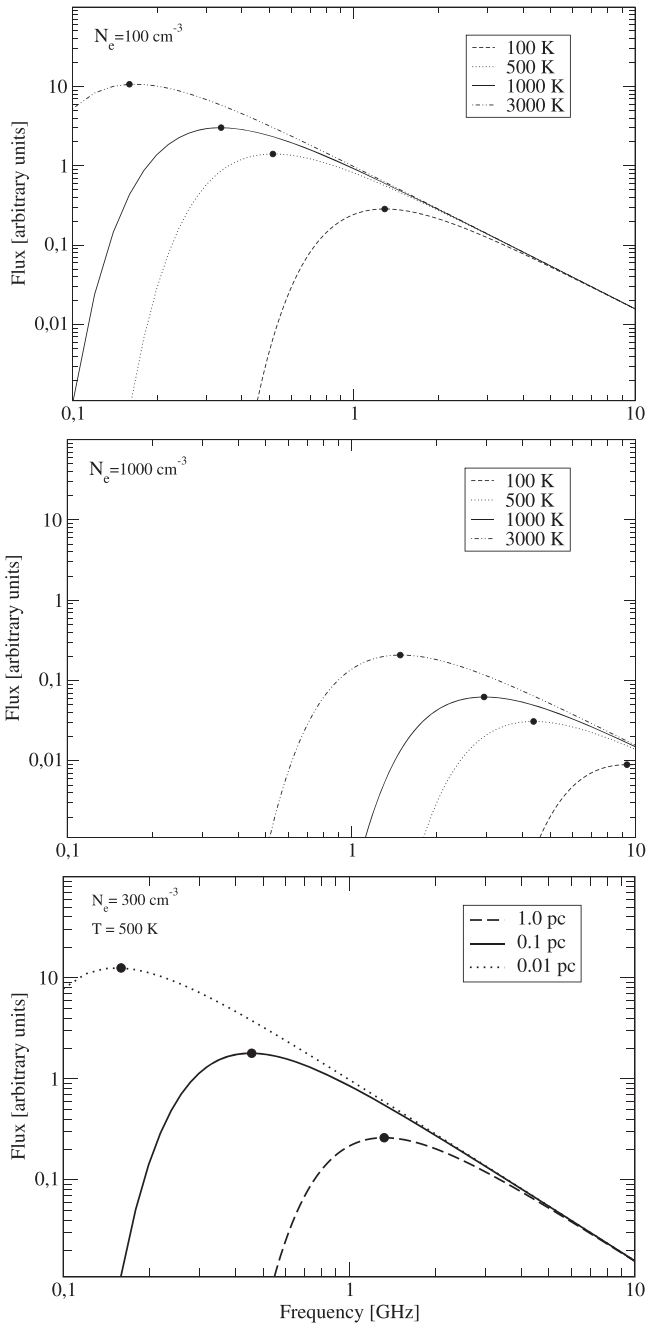

Figure 1. Simulated spectra of a pulsar in the case of the presence of an absorber with a thickness of 1.2 pc. The top panel shows the spectra for a case where the electron density is equal to 100 cm^{-3} and different temperatures of the absorbing electrons. The middle panel shows spectra simulated for the same temperatures of the absorber but the electron density was set to 1000 cm^{-3}. The bottom panel shows the simulated pulsar spectra for various thicknesses of the absorbing region. In this case, the electron density and the electron temperature are assumed to be equal to 300 cm^{-3} and 500 K, respectively.

One can see that under such physical conditions one needs an absorber of about a parsec width to be able to produce absorption that produces a pulsar spectrum that peaks at frequencies close to 1 GHz.

Our calculations have demonstrated that in order to explain the observed GPS of pulsars, one needs an absorber of at least a fraction of a parsec thick, with relatively low temperature (preferably below 1000 K) and with a significant electron number density of the order of a few hundred particles per cm^3. The exact effect of the thermal absorption on the pulsar spectrum obviously depends on the combination of all of these three factors.

2.2. SNR Filaments

Naturally, the question arises of whether, in pulsar environments, we can find some possible absorbers that can fulfill the conditions implicated by our simulations. One of the main problems is connected with the thickness of the absorbing electron-rich material as it is hard to imagine any homogenous cloud of a size of a parsec within a supernova remnant.

When it comes to the observed densities and the electron temperatures, the available data are very limited because it is not easy to measure these quantities. According to Graham et al. (1989) estimations, in the Crab Nebula filaments, the electron density is about 200 cm^{-3}.

The free electrons are partially created by the photoionization of hydrogen atoms in the Nebula and it is easier to measure the number density of hydrogen than that of electrons. Using the observations of ionized nitrogen and oxygen ([N II] and [O III]), Sankrit et al. (1998) estimated that the hydrogen density in the filaments ranged from 1050 to 2218 cm^{-3} and its temperature was very high (over 8000 K). However, it should be mentioned that the Crab Nebula is quite a special case and it is difficult to generalize the results to another SNR.

Much higher densities were observed in very dense filaments of the G11.1-03 supernova remnant where the estimated electron density was even as high as $N_e = 6600 \pm 900$ cm^{-3}, the temperature was about 5000 K, and the thickness of the filament was approximately 0.24 pc Koo et al. (2007).

It follows from all of the above that the filaments in the G11.1-03 SNR are the most promising candidates for the source of the GPS phenomenon. In these filaments, the free electron densities are much higher than the one we used while simulating the spectra shown in the right panel of Figure 1. Even if we assumed a slightly higher electron temperature (than what we used, see Figure 1), the filaments would still provide enough absorption to obtain the spectral peak at gigahertz frequencies. In fact, for this particular filament (Koo et al. 2007), the simulated pulsar spectra peaks at the frequency of 3 GHz, assuming 6600 cm^{-3}, 5000 K, and 0.24 pc for the electron density, the electron temperature, and the thickness, respectively.

The fact that only absorption in the SNR filaments can lead to the appearance of the GPS pulsars naturally explains why most of the SNR-associated pulsars do not show this type of spectrum. It is an observational selection effect since such filaments do not cover a nebula completely, the lines of sight of a very small fraction of pulsars pass through such filaments and, therefore, only these pulsars show the GPS phenomena.

2.3. Isolated GPS Pulsars with PWNs

In this section, we explore the thermal absorption of the radio waves emitted from the pulsar in its PWN. For our purposes, we mostly consider the bow-shock PWNe. There are several reasons why other types of pulsar nebulae can be excluded. For example, the young PWNe (such as the Crab PWN) should be excluded due to very high electron temperatures. As for the spherically symmetric PWNe, they each tend to have a very low thickness.

The shape of the PWN depends mainly on its evolutionary stage. The details of the PWN evolution theory can be found in Gaensler & Slane (2006). Let us summarize it as follows. In the beginning, the shape of practically all PWNe is nearly spherically symmetric and the pulsar is located in the center of its SNR. Later, when the reverse shock of the SNR passes through the PWN, its symmetric shape is disturbed and, after the reverberation phase, the new smaller and often spherically symmetric PWN can be formed. At this evolutionary stage, if the pulsar moves through its SNR with a supersonic speed, the former spherical PWN takes on a cometary appearance. At this stage, the detailed MHD simulations provide significant information about the evolution of the PWNe (see Bucciantini 2014 for the recent review of the MHD simulations).

In our model, the thermal absorption strongly depends on the orientation of the line of sight with respect to the asymmetric bow-shock PWN. The structure of such PWNe can be found, e.g., in Bucciantini (2002, see also our Figure 3). There are three main regions of a PWN (see Figure 3): (1) the free pulsar wind region, (2) the shocked pulsar wind region, and (3) the shocked ISM that is interacting with the shocked pulsar wind material. Since the strength of the free–free absorption depends on N_e^2, we concentrate on the regions (2) and (3) because they can potentially have the highest densities.

Figure 2 presents the outcome of the free–free absorption in the cometary-shaped PWN. For simplicity, we have assumed both density and temperature profiles to be uniform over the regions that contribute to the absorption. These are marked as (2) and (3) in the lower left part of Figure 2 (the structure of the PWN is based directly on Bucciantini 2002). The spectra plots shown in the separate panels present the possible shapes of the apparent pulsar spectra (modified by the absorption) for two different sets of parameters, namely the temperature T and the electron density N_e (the values used are presented in the plots). The panels (a)–(c) in Figure 2 show the apparent shape for three different orientations of the line of sight corresponding to the observers location behind (a), at the side (b), and in front of the bow-shock PWN (c). Since we assume the uniform density and temperature profiles, the thickness of the absorbing region is the only parameter that varies along with the orientation of the line of sight. This quantity can change from a fraction of a parsec (if an observer is in front of the PWN (c)) up to well over a parsec (if an observer is behind the PWN (a)). This thickness significantly influences the optical depth and hence the apparent spectrum of the pulsar that is located in the middle of the PWN. In the case presented in Figure 2 panel (a), the spectrum looks like a GPS with a peak frequency close to 1 GHz, while, in the case presented in panel (b), the spectrum can be interpreted (depending on the observational frequency range) as a pulsar with a "broken spectrum."[3] However, in the case presented in panel (c), the spectrum hardly differs from its intrinsic single power-law spectrum.

The details of the absorption strongly depend on the actual physical parameters of the absorbing electrons. For some sets of parameters, there can be almost no absorption at all regardless of the line-of-sight orientation (see the spectra presented by dotted lines in Figure 2).

The estimates of the electron density in the PWNe are quite rare. The only measurement we could find in the literature is that of the PWN around PSR B1951+32, where Hester & Kulkarni (1989) and Li et al. (2005) estimated the electron density in front of the forward shock to be of the order of $N_e = 50$–$100\ \mathrm{cm}^{-3}$ (from [O III], [S II], and [N II] emission lines). However, it should be mentioned that this value concerns the density of the uncompressed matter outside the shock while, near (or in) the PWN's bow-shock, the density can be larger.

Of course, we realize that our PWN model is quite simplified, and in reality the profiles of both temperature and density may not be uniform. However, we believe that even such a simplified model shows that, in the case of the asymmetric PWN, the pulsar apparent spectrum strongly depends on the line-of-sight orientation and the influence of the nebula can be quite significant. Therefore, even this model is able to explain why most of the GPS pulsars are found in the PWNe, while, at the same time, a large fraction of pulsars in the PWNe does not show any kind of spectral deviation.

2.4. Sgr A* Radio-magnetar

As we mentioned in the Introduction, Kijak et al. (2013) demonstrated that the spectra of two radio-magnetars seem to exhibit the GPS behavior with the peak frequency of a few gigahertz (5.0 and 8.3 GHz for SGRs J1550–5418 and J1622–4950, respectively). Kijak et al. (2013) suggested that the thermal absorption of radio waves is responsible for the GPS appearance in the case of the radio-magnetars in the same way as it is in the case of the normal GPS pulsars.[4] However, the reason for the very high peak frequencies is still unclear. It should be mentioned that there is a lack of normal GPS pulsars with such high peak frequencies. That may be explained by observational selection effects because it is very difficult to find such objects in the usual pulsar search surveys, which are mostly performed at frequencies at which the GPS-pulsars with high peak frequencies could be very faint.

Another, and probably the most famous (at least nowadays) radio-magnetar, SGR J1745–2900, also known as the Sagittarius A* magnetar (due to its location at the center of the Milky Way) was discovered by the *Swift* Telescope on 2013 April 25 (Kennea et al. 2013). The *NuSTAR* observation on 2013 April 26 found the object variability with the period ~3.76 s (Mori et al. 2013). These observations led to an identification of this source as a new magnetar undergoing an outburst. Later, the Sgr A* magnetar was observed by radio-telescopes and consequently was first detected at higher radio frequencies and later at frequencies as low as 1.5 GHz. The flux density measurements (among other data) were performed by several observing groups using several telescopes around the world: the Effelsberg radio telescope, the VLA, the telescopes at Nançay, Jodrell Bank, Green Bank, and Parkes (see Eatough et al. 2013; Rea et al. 2013 and references therein).

Further observations made by the Australia Telescope Compact Array (ATCA) provided data for the magnetar radio spectrum for two epochs: 2013 May 1 and 31 and for two frequency ranges: from 4.5 to 8 GHz and from 16 to 20 GHz (Shannon & Johnston 2013). Figure 3 presents (in log–log scale) the SGR J1745–2900 spectra obtained for these two epochs: the circles denote the measurements from May 1, while the triangles denote May 31 data (values taken from Figure 4 by Shannon & Johnston 2013). The top panel in Figure 3 shows fits to the whole data set, which was based on the

[3] Broken spectrum is a class of pulsar spectra that is often morphologically described by two power laws, with the lower frequency slope being flatter.

[4] Let us note that a mechanism for radio emission of magnetars should not differ essentially from that of the normal pulsars (Szary et al. 2015).

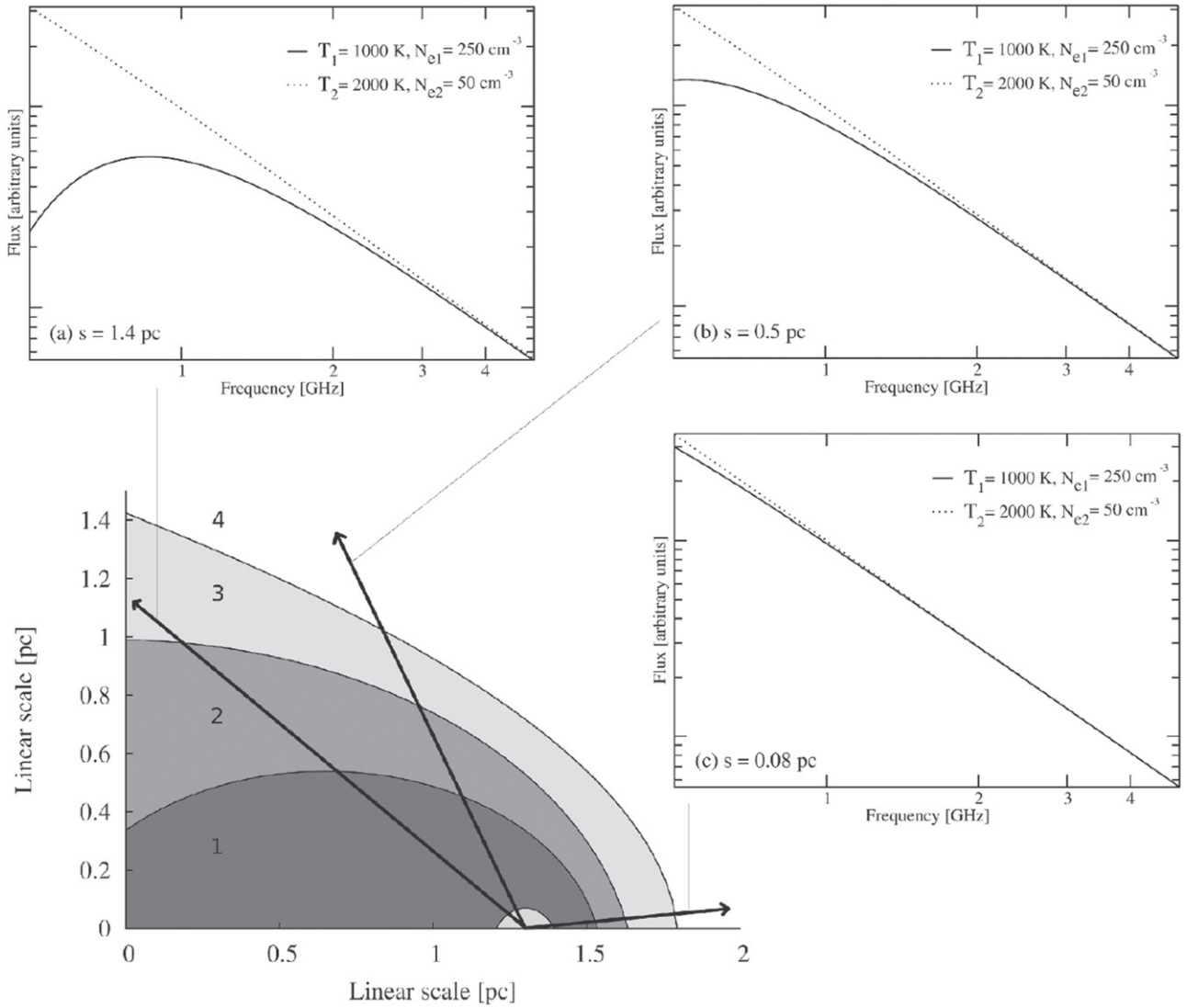

Figure 2. Schematic view of the bow-shock PWN (based on the MHD simulations Bucciantini 2002). The numbered PWN regions are (1) the free relativistic pulsar wind region, (2) the shocked pulsar wind region, (3) the shocked ISM interacting with the shocked pulsar wind material, and (4) the ISM. The termination shock is located between (1) and (2) and the forward shock is located between (3) and (4). The simulated apparent pulsar spectra for various orientations of the line of sight are presented in the subpanels; each of them shows two spectra obtained for different sets of physical parameters. Obviously, in some parameter domains, the same pulsar-PWN system can yield a different pulsar spectrum depending on the direction of the line of sight (for a detailed discussion see the text).

observations in two frequency bands. The data from May 1 definitely do not resemble a typical pulsar spectrum (a single power law) and thus suggest the possible GPS case. We have performed a log-parabolic fit to the data (i.e., the fitted function was $S(\nu) = 10^{(a \log^2 \nu + b \log \nu + c)}$, see Kuzmin & Losovsky 2001) and, as a result, we have found a possible maximum in the spectrum at 6.3 GHz. This value seems to be similar to the peak frequencies that were found for the other two radio-magnetars mentioned above. We have attempted to fit a single power-law spectrum to the data obtained on May 31 because a slight bend noticeable in the data is not big enough to indicate the maximum of the spectrum. As a result, we have obtained a spectral index of $\alpha = -1.18 \pm 0.04$ but as one can see in the left panel of Figure 3 the power law (indicated by the dashed line) fits the lower frequency band almost perfectly, while, for the higher frequency band, the fit is not so good.

The reason why the fit at the high frequency band deviates from the data points is the chosen fitting method, namely the so-called weighted fitting method. As the uncertainties of the flux measurements at the higher frequency were much larger than those at the lower frequencies, the fit weights of the high frequency data were much lower than those of the lower frequency data. On the other hand, the distribution of the 16–20 GHz band data points (with respect to the fit line, see the middle panel of Figure 3) is not random and show an apparent trend indicating a steeper slope. This is why we have performed the fitting separately for the lower and higher frequency ATCA bands. The obtained fits are presented in the right panel of Figure 3. For the data from May 1, we obtained a spectral slope of -0.01 ± 0.08 for the 4.5–8.5 GHz band and -3.42 ± 0.57 for the 16–20 GHz range. Similar fits have been performed for the May 31 data yielding $\alpha = -0.98 \pm 0.03$ at lower frequencies and $\alpha = -2.95 \pm 0.50$ at higher frequencies. As one can see in Figure 3, the two spectral slopes (obtained by the data from May 1 and 31) in the higher band are almost the same for both epochs (the slops coincide within the error bars), while, in the lower frequency, the spectra apparently differ from each other. It is obvious that the pulsar was significantly

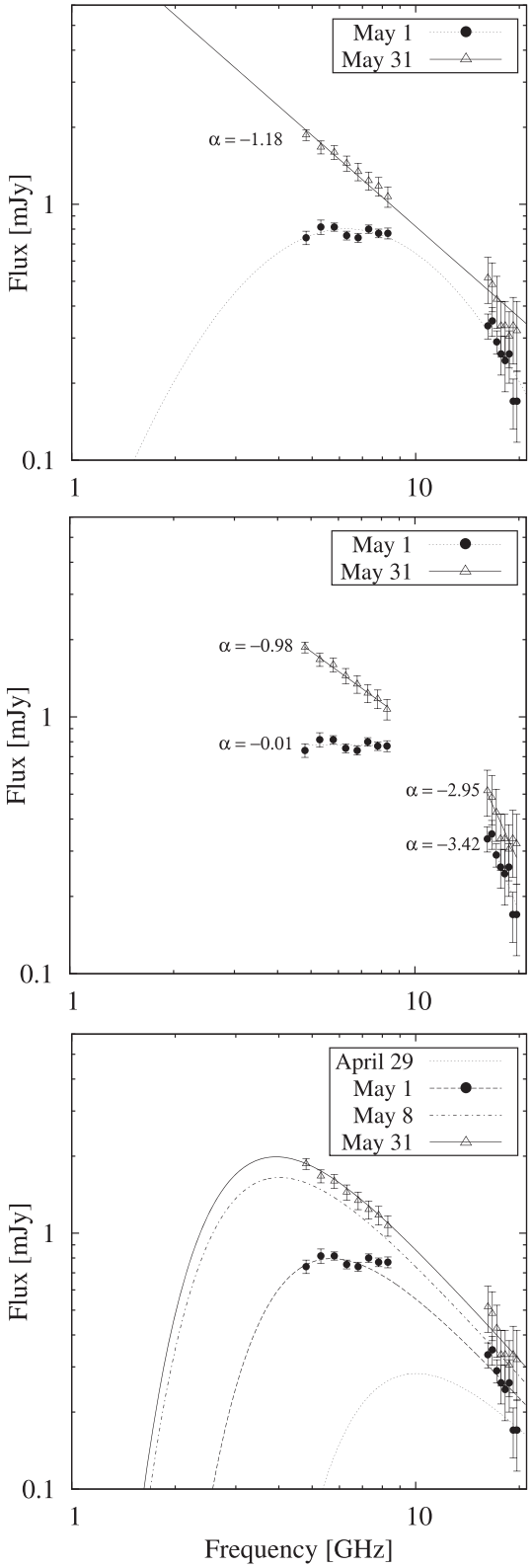

Figure 3. Spectra of the radio-magnetar SGR J1745–2900. Full dots denote the 2013 May 1 observations, empty triangles—the 2013 May 31 measurements (all values are taken from Figure 4 in Shannon & Johnston 2013). The top panel shows our fits to the entire frequency range: the parabolic fit to the May 1st data and a power-law fit for the May 31 observations. The middle panel shows two power-law fits (i.e., a "broken spectra" fits) that are performed separately for the two frequency bands used in the observation. The bottom panel shows the results of the absorption model fits for the observed data, as well as the spectra modeled for April 29 and May 8 (see Section 2.4 for details of the model).

weaker during the first observation, but also the spectrum on that date seems to be flat, while, a month later, it is definitely steeper.

We believe that this kind of behavior may be caused by a thermal free–free absorption in the wind nebula around the Sgr A* radio-magnetar. On 2013 May 1, the optical depth of the nebula was higher, hence the absorption was stronger, due to the higher electron density. Therefore, the radio-magnetar exhibited the GPS behavior. However, a month later, the optical depth decreased due to dissipation of the absorbing material and consequently the absorption became weaker, but probably still observable, on 2013 May 31.

Since the free–free absorption affects the higher observing frequencies to a much lower extent, the slope in the higher frequency band stays unchanged. At the same time, the flux at lower frequencies gets stronger and, in the 4.5–8.5 GHz band, the spectra becomes sloped, which can indicate that the absorption decreases.

The explanation given above, as well as the idea of the spectral evolution in general, does not contradict the other observations using various radio-telescopes (see, e.g., Eatough et al. 2013; Rea et al. 2013). These observations, which were carried out over a wide range of epochs, indicated that after a few days of unsuccessful attempts the pulsar was first detected at higher frequencies. Additionally, despite various attempts, the first detection at 1.5 GHz became possible only in mid-May, i.e., two to three weeks after the outburst from April 25. It should be mentioned that the observations carried out on different dates cannot be used for obtaining the spectra because it varies considerably over several days.

We can speculate on the cause of the decrease of the absorption, assuming that we deal with the case of free–free absorption. We find it unlikely that the rate of absorption would change due to the temperature variations. If it were so, the temperature would have to increase but there is no apparent reason for a growth of the temperature. Another obvious way to decrease absorption is to decrease the electron density because the absorption strength is very sensitive to density variations. We can suggest that the simplest possible explanation for the SGR J1745–2900 radio spectra evolution is the absorption in the electron material ejected during the magnetar outburst.

Initially, the density of absorbing material was so high that even at the higher observing frequencies the radio pulsations were undetectable. If one assumes that the ejected material expands in the form of a spherical shell and with a constant velocity, the density decreases with distance as $1/r^2$ (or with time as $1/t^2$) the optical depth of the absorbing medium falls even faster than the density ($1/r^4$). Therefore, it was possible to detect the radio-magnetar in just a few days after the outburst at higher radio frequencies, while, at lower frequencies, detection became possible only in a few weeks. One can argue that the decrease of the optical depth due to the decreasing density might, at least to some extent, be compensated by the decrease of the temperature of the ejecta. However, the optical depth is much more sensitive to the variation of the density than to that of the temperature (see Equation (2)). In addition we have assumed that the cooling of the matter is an adiabatic process (because it is usually assumed in the cases of outbursts and explosions, for example, in the supernovae models) which usually leads to a linear drop in temperature with distance ($T \sim 1/r$). Thus, the net effect should be a decrease of the

optical depth that leads to the decrease of absorption and to the shift of the peak frequency toward lower frequencies.

In the case of PSR J1745–2900, it is impossible to develop a detailed model based only on the observational data. To explain the amount of absorption responsible for the appearance of the spectra, one needs information about the electron density, temperature, and thickness of the absorber. The only parameter that could be associated with the observational data is the initial temperature of the ejecta, which, in our model, is assumed to be the same as the temperature inferred from the X-ray spectrum of the outburst. As for the detailed model of the relation between these temperature(s), it is still under debate. These data, based on the X-ray spectrum observed during the outburst (see Kennea et al. 2013) indicate two different temperatures of the ejecta: the first, 10^8 K, was observed on April 25 during the discovery observation of the outburst and the second, lower one, 10^7 K, was determined based on the integrated data obtained during very long observation sessions after the outburst. In our model, we used the latter value. In our model, the temperature of the ejecta decreases linearly with time. However, it cannot decrease indefinitely (if that were the case, then on May 1, just six days after the outburst, it would drop to 100 K). One has to remember that this magnetar is located in a densely populated region of the galactic center and the electron gas should be always heated by the background radiation, just as it is in a typical H II region. For typical ionized regions in the galactic center, the electron temperature is in the range of 5000 to 7000 K (Afflerbach et al. 1996). Therefore, we have adopted 5000 K as the lowest possible temperature of the ejecta, i.e., in our model the temperature never drops below this value. As for the other parameters that influence absorption, we cannot decouple the value of the electron density from the thickness of the expanding spherical layer since we do not have any observational data for these parameters. Hence, we have decided to assume the initial value of the electron density and fit the model to the observational data by adjusting the thickness of the absorber.

While trying to model both the May 1 and 31 spectra, we have come to the conclusion that any absorption that enables us to explain the shape of the May 1 spectrum will completely disappear in 31 days. Hence, in order to explain the shape of the May 31 spectrum, we have introduced constant absorption in addition to the expanding ejecta. This idea was strengthened by the results from Pennucci et al. (2015), who observed the Sgr A* magnetar using the Green Bank Telescope. The shape of the spectra they obtained 100 days after the outburst still shows what might be an indication of thermal absorption. Our initial assumption was that such an external absorption may be provided by either the interstellar medium and/or some kind of residual PWN around the radio-magnetar, which may exist due to the previous outbursts of the source.[5] However, as we discuss below, this is not the case.

Since we have no information about the physical parameters of this external absorber, we have decided to explore two possibilities. One possibility is to assume that the absorption happens in a cold medium, such as a dense (and partially ionized) molecular cloud, which is similar to the SNR filament we discussed above. If we assume the temperature of a cloud to be 200 K and its thickness to be about 1 pc, then the electron density in the cloud should be close to 500 cm^{-3} in order to satisfy the May 31 absorption. On the other hand, if we assume that there is no such cloud in the magnetar's line of sight and the absorption happens in a hot medium (5000 K), then, in order to satisfy the observed absorption, the thickness of the absorbing medium should be about 0.15 pc and the electron density should be about 10^4 cm^{-3}. Let us note that this value is typical for the galactic center H II regions, see Genzel et al. (1995). The fit (which is obviously the same for both of these sets of parameters) to the spectrum is shown in the bottom panel of Figure 3 by the solid line. It is worth mentioning that, to obtain this specific spectrum, one can use many sets of parameters and the set mentioned above represents only some of the possibilities. The validity of these parameter sets is discussed later in this section based on other observable properties of the magnetar.

In our modeling of the May 1 spectrum, the temperature of the ejecta is already the lowest allowable value, 5000 K. Thus we have to use some reasonable values for the initial electron density and the geometrical thickness of the shell. Taking into account the external absorber, we can obtain the shape of the May 1 spectrum if we assume that the electron density is $N_e \simeq 2 \times 10^5$ cm^{-3} and the geometrical thickness of the shell is close to 0.7 light-days (or 5×10^{-4} pc). These values seem quite reasonable for the May 1 (six days after the initial outburst) conditions. The value $N_e = 2 \times 10^5$ cm^{-3} requires the initial (i.e., at the stellar surface) electron density to be equal to 5×10^4 of the Goldreich–Julian number density, which is estimated as 3×10^{12} cm^{-3} at the surface of this radio-magnetar. The value used for the thickness of the ejecta can be reached if the thermal spread of the electrons in the ejecta is about 10% of the average speed of particles. However, it should be remembered that this thickness is closely bound to the assumed initial density and, if the density is lower, one will need to increase the thickness of the absorber significantly in order to explain the observed effect.

The resulting spectrum is shown in the bottom panel of Figure 3. Let us also note that to satisfy the shape of the spectrum we have to assume that the intrinsic radio spectrum of the magnetar has a spectral of −1.5. This value is significantly lower than the one suggested by the observational data from the higher frequency band (compare the middle panel of Figure 3). However, the use of the steeper intrinsic spectrum results in a much sharper peak in the spectrum after applying the absorption. Thus, it makes our model unable to explain the almost flat spectrum in the lower frequency band of the May 1 data. It should be mentioned that the physical parameters of the absorbing ejecta quoted above represent only one of the possible combinations that can explain the observed absorption.

After fitting our model to the data, we have used this model to estimate the shape of the Sgr A* magnetar spectra for other epochs for the purpose of showing the spectrum evolution. In the bottom panel of Figure 3, besides the curves fitted to the data, we have also presented the modeled spectra for April 29 (four days after the initial outburst) and May 8 (two weeks later). This evolution can easily explain why the radio magnetar was not detectable at lower radio frequencies (i.e., from 1 to 3 GHz range) for almost two weeks after the outburst.

It is worth mentioning that, as a by-product of our model, we have the ability to estimate the contribution made by the

[5] The possibility of the existence of such a PWN around the Sgr A* magnetar was recently discussed by Tong (2014) who also stated that the PWN would be undetectable for the current telescopes due to an extremely large distance to the source which is located in the galactic center.

absorber to the magnetar's dispersion measure. The DM of PSR J1745–2900 was reported to be in the range of 1650 to 1830 pc cm^{-3} (various authors quote different values, see Eatough et al. 2013; Rea et al. 2013; Shannon & Johnston 2013). Assuming the homogenous density distribution, and using the expression for the DM, $\Delta \mathrm{DM} = N_e d$ (here d is the thickness of the absorber in parsecs), we can estimate the amount of DM added by the ejecta to the magnetar's DM for the May 1 conditions. This additional value turns out to be of about 100 pc cm^{-3} and obviously drops with time due to the decrease in the electron density. Thus, this value is smaller than the discrepancy between the DM values given by various authors. Additionally the published DMs are usually given without the exact epoch of the measurement.

We can also estimate the contribution to the total DM from the material that provides what we call the external absorption. If we assume that this absorption happens in the cold molecular cloud (with the thickness of 1 pc, $N_e = 500$ cm^{-3} and $T = 200$ K), which is one of the possibilities suggested earlier, then its contribution to the total DM can be estimated as 500 pc cm^{-3}, which is significantly greater than that of the ejecta. We believe that this can explain the observed value of the DM as compared to the DMs of other pulsars that lie close to, or behind, the galactic center. The DMs of these pulsars rarely exceed 1200 pc cm^{-3}.

On the other hand, we know that the magnetar is located extremely close to the galactic center (0.09 pc) and the surrounding ISM resembles a hot H II region (the second set of parameters we discussed earlier: the thickness of 0.15 pc, $T = 5000$ K and $N_e = 10^4$ cm^{-3}). Therefore, its contribution to the total DM would be of the order of 1500 pc cm^{-3}, which is clearly too high. Since the above-mentioned parameters of the absorbing region are only tentative, we can freely adjust them. Let us note that the optical thickness $\tau \propto d\, N_e^2$ and the contribution to the total DM is equal to dN_e. Thus, higher electron densities and smaller sizes are needed in order to provide the same observed absorption, but with a smaller contribution to the total DM, i.e., an absorber with $N_e = 1.8 \times 10^4$ cm^{-3} and the thickness of 0.05 pc would contribute only 900 pc cm^{-3} to the total DM, assuming the same temperature of 5000 K. The further decrease of the DM contribution requires very small sizes of the absorber region, which seems to be rather unlikely. Therefore, we believe that a cold ISM cloud is the most likely candidate for an absorber in this case.

Obviously, our calculations of the contributions to the magnetar's DM provided by both the ejecta and the external absorber are based on specific density and thickness estimates that follow from our model. Since a number of different sets of parameters can satisfy the observed absorption and the resulting DM contribution is variable, these calculations should be considered to be rough estimates.

To summarize our discussion on the Sgr A* radio magnetar, we can explain, at least to some extent, the basic properties of the observed evolution of its radio spectrum by the free–free absorption in the expanding electron cloud that was ejected during the outburst. However, our ability to perform a detailed study is limited due to the sparseness of observations (i.e., multi-frequency flux density measurements) because we have somewhat reasonable spectra for only two epochs. Nevertheless, we believe that our model provides an adequate explanation of the observational data. Also, the PSR J1745–2900 radio magnetar is thus far the only one for which we have relatively detailed spectra for certain epochs (thanks to the data from Shannon & Johnston 2013). Unfortunately, we cannot apply our model to the spectra of the other two GPS magnetars since their spectral data are much more sparse. We can only hope that in the future observations of the radio-magnetar outbursts the assessment of the evolution of the spectrum and the DM variations, especially within the first several days, will become one of the priorities.

3. CONCLUSIONS

In this paper, we have explored the possibility that the GPS (observed in a number of pulsars and radio-magnetars) may be caused by the thermal free–free absorption in the electron mater of the neutron star surroundings (see also Kijak et al. 2011b, 2013). Using the simplified model, which assumes a constant density and temperature profiles in the absorbing media, we were able to simulate the spectra of pulsars that resemble the spectra of the known GPS objects at least qualitatively. We have discussed several possible scenarios and geometries of the pulsar surroundings that can provide the absorption that makes a pulsar spectrum peak at the frequencies 1 GHz and above. One of these scenarios is the case of very dense filaments in the SNRs, and we have shown that at least some of the observed filaments are dense and possibly cold enough to affect the pulsar spectrum in a desired way. The fact that such an absorption indeed requires the most dense (and thus obviously relatively small) parts of an SNR to be involved may explain why not all pulsars associated with SNR show the GPS signature in their spectrum.

Another possibility we have explored is the thermal absorption in the PWN, and our simulations show that these objects may indeed be a cause of the GPS if the geometry is favorable, i.e., the same kind of PWN depending on the orientation of the line of sight may or may not provide enough absorption to cause the pulsar spectrum to peak at a few gigahertz. We have found that in order to observe the significant absorption in the cometary-shaped bow-shock PWN, the observer should be located behind the PWN (see panel (a) of Figure 2). At the same time, this geometrical dependence may explain why some of the PWN associated pulsars do not exhibit a GPS phenomenon. Although beyond the geometry the free–free absorption may also strongly depend on the physical properties of a PWN, and hence also on its evolutionary phase.

The other two cases that we have studied include the spectral evolution. In the case of the binary system PSR B1259–63/LS2883 (discussed in detail by Dembska et al. 2012) the evolution occurs due to the pulsar orbital motion that changes the orientation of the line of sight with regard to the absorbing region and, therefore, the absorption rate increases significantly when the pulsar moves deeper in the dense stellar wind of its Be-star companion. In the case of the Sgr A* radio-magnetar (which would be the third magnetar with a GPS) the spectral evolution is caused by the free–free absorption of the magnetar radio emission in the electron material ejected during the outburst. The ejecta expands with time and, consequently, the absorption rate decreases and the shape of the spectrum changes in such a way that the peak frequency shifts toward the lower radio frequencies.

This work was supported by grants DEC-2012/05/B/ST9/03924 and DEC-2013/09/B/ST9/02177 of the Polish National Science Centre. We are grateful to the anonymous referee for many constructive comments that helped us to significantly improve this paper.

REFERENCES

Afflerbach, A., Churchwell, E., Acord, J. M., et al. 1996, ApJ, 106, 423
Bates, S. D., Lorimer, D. R., & Verbiest, J. P. W. 2013, MNRAS, 431, 1352
Bucciantini, N. 2002, A&A, 387, 1066
Bucciantini, N. 2014, IJMPS, 28, 1460162
Dembska, M., Kijak, J., Jessner, A., et al. 2014, MNRAS, 445, 3105
Dembska, M., Kijak, J., Koralewska, O., Lewandowski, W., & Melikidze, G. 2012, arXiv:1212.6630
Eatough, R. P., Falcke, H., Karuppusamy, R., et al. 2013, Natur, 501, 391
Gaensler, B. M., & Slane, P. O. 2006, ARA&A, 44, 17
Genzel, R., Eckart, A., & Krabbe, A. 1995, in Seventeeth Texas Symp. on Relativistic Astrophysics and Cosmology 759, Annals of the New York Academy of Sciences, ed. H. Böhringer, G. E. Morfill & J. E. Trümper (New York: New York Acad. Sci.), 38
Graham, J. R., Wright, G. S., & Longmore, A. J. 1989, in Infrared Spectroscopy in Astronomy, ed. E. Böhm-Vitense (ESA SP-290; Noordwijk: ESA), 169
Hester, J. J., & Kulkarni, S. R. 1989, ApJ, 340, 362
Hester, J. J., Stone, J. M., Scowen, P. A., et al. 1996, ApJ, 456, 225
Kennea, J. A., Burrows, D. N., Kouveliotou, C., et al. 2013, ApJL, 770, L24
Kijak, J., Dembska, M., Lewandowski, W., Melikidze, G., & Sendyk, M. 2011b, MNRAS, 418, L114
Kijak, J., Gupta, Y., & Krzeszowski, K. 2007, A&A, 462, 699
Kijak, J., Lewandowski, W., Maron, O., Gupta, Y., & Jessner, A. 2011a, A&A, 531, A16
Kijak, J., Tarczewski, L., Lewandowski, W., & Melikidze, G. 2013, ApJ, 772, 29
Koo, B.-C., Moon, D.-S., Lee, H.-G., Lee, J.-J., & Matthews, K. 2007, ApJ, 657, 308
Kramer, M., Xilouris, K. M., Lorimer, D. R., et al. 1998, ApJ, 501, 270
Kuzmin, A. D., & Losovsky, B. Ya. 2001, A&A, 368, 230
Li, X. H., Lu, F. J., & Li, T. P. 2005, ApJ, 628, 931
Lorimer, D. R., Yates, J. A., Lyne, A. G., & Gould, D. M. 1995, MNRAS, 273, 411
Maron, O., Kijak, J., Kramer, M., & Wielebinski, R. 2000, A&AS, 147, 195
Mori, K., Gotthelf, E. V., Zhang, S., et al. 2013, ApJL, 770, L23
Pennucci, T. T., Possenti, A., Esposito, P., et al. 2015, ApJ, in press (arXiv:1505.00836)
Rea, N., Esposito, P., Pons, J. A., et al. 2013, ApJL, 775, L34
Rohlfs, K., & Wilson, T. L. 2004, Tools of Radio Astronomy (Berlin: Springer)
Sankrit, R., Hester, J. J., Scowen, P. A., et al. 1998, ApJ, 504, 344
Shannon, R. M., & Johnston, S. 2013, MNRAS, 435, L29
Sieber, W. 1973, A&A, 28, 237
Szary, A., Melikidze, G., & Gil, J. 2015, ApJ, 800, 5
Tong, H. 2014, RAA, in press (arXiv:1403.7898)